Article

# Atomic Force Microscopy Studies of DNA-Wrapped Carbon Nanotube Structure and Binding to Quantum Dots

Jennifer F. Campbell, Ingrid Tessmer, H. Holden Thorp, and Dorothy A. Erie

*J. Am. Chem. Soc.*, **2008**, 130 (32), 10648-10655 • DOI: 10.1021/ja801720c • Publication Date (Web): 16 July 2008



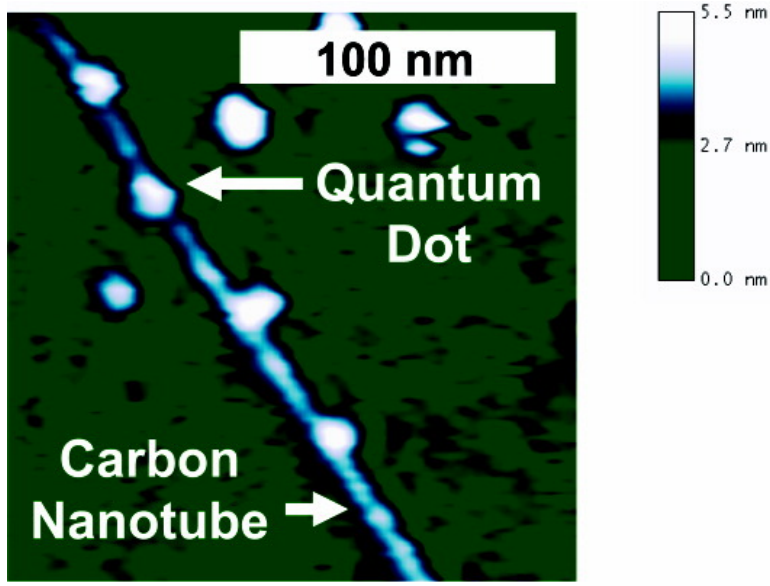


## More About This Article

Additional resources and features associated with this article are available within the HTML version:

- Supporting Information
- Access to high resolution figures
- Links to articles and content related to this article
- Copyright permission to reproduce figures and/or text from this article

View the Full Text HTML

J|A|C|S
ARTICLES

Published on Web 07/16/2008

# Atomic Force Microscopy Studies of DNA-Wrapped Carbon Nanotube Structure and Binding to Quantum Dots

Jennifer F. Campbell, Ingrid Tessmer,† H. Holden Thorp, and Dorothy A. Erie*,‡

*Department of Chemistry, University of North Carolina at Chapel Hill, Chapel Hill, North Carolina 27599*

Received March 7, 2008; E-mail: derie@unc.edu

***Abstract:*** Single-stranded DNA is an effective noncovalent dispersant for individual single-walled carbon nanotubes (CNTs) in aqueous solution, forming a CNT−DNA hybrid material that has advantages for CNT separations and applications. Atomic force microscopy (AFM) reveals a regular pattern on the surface of CNT−DNA. We found this pattern to be independent of the length and sequence of the wrapping DNA, yet different from the structures observed for CNTs dispersed with sodium dodecyl sulfate in the absence of DNA. We wrapped CNTs with thiol-modified DNA to form stable conjugates of CNT−DNA and core/shell CdSe/ZnS quantum dots; AFM imaging of these conjugates identified for the first time the location of DNA on the CNT−DNA nanomaterial. Our results suggest that the AFM pattern of CNT−DNA is formed by helical turns (∼14-nm pitch) of wrapped DNA strands that are closely arranged end-to-end in a single layer along the CNT. This work demonstrates the useful functionalization of CNTs with quantum dots in a manner that avoids direct, destructive modification of the CNT surface and suggests nearly complete surface coverage of the nanotubes with DNA.

## Introduction

Single-walled carbon nanotubes (CNTs) inspire multidisciplinary interest, with promising roles in nanoelectronics[1] and biology[2–4] and value as an analytical tool.[5] However, applications are encumbered by the poor solubility of unmodified CNTs in aqueous and organic solvents, which causes nanotube aggregation and alters their optical-electronic properties. Accomplishing the water solubilization of CNTs has elucidated important nanotube properties, including their solution near-infrared fluorescence[6–8] and electrochemistry,[9,10] and is essential to the development of CNT biological applications. Aqueous CNT solutions have been formed through both chemical modification of CNTs[11] and noncovalent interactions with CNTs such as the adsorption of surfactants[6] and polymer-wrapping.[12–14] Covalent functionalization negatively affects CNT electrical and optical properties;[15,16] therefore, noncovalent modification has the advantage of providing CNTs with water solubility while preserving their remarkable properties.

Single-stranded (ss)DNA acts as an effective noncovalent dispersant for the water solubilization of CNTs.[17] Ultrasonication facilitates the separation of aggregated CNTs, producing individually solubilized nanotubes wrapped with DNA (CNT−DNA).[17] The dissolution is accomplished because the aromatic nucleotides of DNA interact via $\pi$-stacking[17,18] with the hydrophobic CNT surface, while the polyanionic DNA backbone confers water solubility. The strength of the binding interactions between CNTs and ssDNA is demonstrated by the ability of the DNA to disrupt the strong intertube interactions responsible for CNT aggregation into bundles.

This CNT−DNA nanomaterial has been used to study CNT optical-electronic properties,[9,10,19,20] improve nanotube field

† Present address: Rudolf-Virchow Zentrum für Experimentelle Biomedizin, Universität Würzburg, Versbacher Str. 9, 97078 Würzburg, Germany.

‡ Curriculum in Applied and Materials Sciences.

(1) Colbert, D. T.; Smalley, R. E. *Trends Biotechnol.* **1999**, *17*, 46–50.
(2) Barone, P.; Baik, S.; Heller, D. A.; Strano, M. S. *Nat. Mater.* **2005**, *4*, 86–92.
(3) Heller, D. A.; Baik, S.; Eurell, T. E.; Strano, M. S. *Adv. Mater.* **2005**, *17*, 2793–2799.
(4) Kam, N. W. S.; O'Connell, M.; Wisdom, J. A.; Dai, H. *Proc. Natl. Acad. Sci. U.S.A.* **2005**, *102*, 11600–11605.
(5) Trojanowicz, M. *Trends Anal. Chem.* **2006**, *25*, 480–489.
(6) O'Connell, M. J.; Bachilo, S. M.; Huffman, C. B.; Moore, V. C.; Strano, M. S.; Haroz, E. H.; Rialon, K. L.; Boul, P. J.; Noon, W. H.; Kittrell, C.; Ma, J.; Hauge, R. H.; Weisman, R. B.; Smalley, R. E. *Science* **2002**, *297*, 593–596.
(7) Bachilo, S. M.; Strano, M. S.; Kittrell, C.; Hauge, R. H.; Smalley, R. E.; Weisman, R. B. *Science* **2002**, *298*, 2361–2366.
(8) Strano, M. S.; Doorn, S. K.; Haroz, E. H.; Kittrell, C.; Hauge, R. H.; Smalley, R. E. *Nano Lett.* **2003**, *3*, 1091–1096.
(9) Zheng, M.; Diner, B. A. *J. Am. Chem. Soc.* **2004**, *126*, 15490–15494.
(10) Napier, M. E.; Hull, D. O.; Thorp, H. H. *J. Am. Chem. Soc.* **2005**, *127*, 11952–11953.
(11) Pompeo, F.; Resasco, D. E. *Nano Lett.* **2002**, *2*, 369–373.
(12) O'Connell, M. J.; Boul, P.; Ericson, L. M.; Huffman, C.; Wang, Y.; Haroz, E.; Kuper, C.; Tour, J.; Ausman, K. D.; Smalley, R. E. *Chem. Phys. Lett.* **2001**, *342*, 265–271.
(13) Star, A.; Steuerman, D. W.; Heath, J. R.; Stoddart, J. F. *Angew. Chem., Int. Ed.* **2002**, *41*, 2508–2512.
(14) Dieckmann, G. R.; Dalton, A. B.; Johnson, P. A.; Razal, J.; Chen, J.; Giordano, G. M.; Munoz, E.; Musselman, I. H.; Baughman, R. H.; Draper, R. K. *J. Am. Chem. Soc.* **2003**, *125*, 1770–1777.
(15) Bahr, J. L.; Yang, J.; Kosynkin, D. V.; Bronikowski, M. J.; Smalley, R. E.; Tour, J. M. *J. Am. Chem. Soc.* **2001**, *123*, 6536–6542.
(16) Banerjee, S.; Hemraj-Benny, T.; Wong, S. S. *Adv. Mater.* **2005**, *17*, 17–29.
(17) Zheng, M.; Jagota, A.; Semke, E. D.; Diner, B. A.; McLean, R. S.; Lustig, S. R.; Richardson, R. E.; Tassi, N. G. *Nat. Mater.* **2003**, *2*, 338–342.
(18) Hughes, M. E.; Brandin, E.; Golovchenko, J. A. *Nano Lett.* **2007**, *7*, 1191–1194.
(19) Chou, S. G.; et al. *Chem. Phys. Lett.* **2004**, *397*, 296–301.


**10.1021/ja801720c CCC: $40.75** 

effect transistors,[21] and construct chemical sensors.[22] Wrapping CNTs with DNA also allows them to be chromatographically sorted by nanotube length, diameter, and (*n*,*m*) type (where *n* and *m* together describe the diameter and chirality, and thus the electronic character, of an individual CNT).[23–26] Since the heterogeneity of CNT samples is one of the biggest obstacles to nanotube study and application, these achievements toward purifying CNTs highlight the usefulness of CNT−DNA hybrids. Furthermore, the use of the DNA biomolecule to dissolve CNTs makes it possible to apply molecular biology tools to manipulate CNTs and to utilize the sequence-specific nature of DNA base pairing to direct the assembly of CNTs into useful architectures.[27,28]

In these CNT−DNA separation and assembly applications, the structure of DNA on the CNTs is an important feature that is not entirely understood. Models of the CNT−DNA hybrids suggest that helical wrapping of DNA around CNTs is possible, but the flexibility of ssDNA allows for a variety of possible structures.[17,29,30] The structure and stability of DNA on the CNT surface is predicted to be influenced by the electronic and physical characteristics of each nanotube,[29,31,32] and this connection between intrinsic nanotube properties and the DNA wrapping structure plays an important role in the separation of CNT−DNA by CNT diameter and electronic character.[23,24,32] Since the separation of CNTs into homogeneous samples is critical to most of their proposed applications, further investigation of the CNT−DNA structure is expected to prove valuable.

Here, we employed atomic force microscopy (AFM) to determine the structure of DNA in CNT−DNA. AFM measurements suggest a model of helically wrapped oligonucleotides that are closely arranged along the entire CNT in a single layer. Each turn of the DNA around the CNT generates a peak in the CNT−DNA height measured by AFM, forming a regular pattern on the nanotube surface. This analysis was supported by imaging CNTs wrapped with oligonucleotides of different lengths and by quantum dot (QD) labeling of the wrapping DNA, which enabled us to identify the location of the individual oligonucleotides on the nanotube surface. The impact of the oligonucleotide sequence was also investigated, and CNT−DNA was compared to CNTs dispersed with sodium dodecyl sulfate (SDS) in the absence of DNA. The insight gained into the organization of DNA on CNT−DNA is anticipated to benefit the future use of this nanomaterial in the study of solution nanotube properties and in the separation of CNTs by (*n*,*m*) type.

## Experimental Section

**AFM.** AFM was performed in air using a Nanoscope IIIa microscope (Veeco Instruments, Santa Barbara, CA) in tapping mode to simultaneously collect height and phase data. Images of 1−2 $\mu$m size were collected at a 1−3 Hz scan rate and 512 × 512 pixel resolution. AFM cantilevers were Pointprobe Plus tapping mode silicon probes (Agilent Technologies, Tempe, AZ) with an ∼170 kHz resonance frequency.

CNTs (CoMoCAT process,[33] SouthWest NanoTechnologies, Norman, OK) were wrapped with ssDNA (MWG-Biotech, High Point, NC) in a series of tip-sonication, centrifugation, and purification steps modified from the literature[17] (see Supporting Information). CNT−DNA solutions (2.7 mg/L or ∼16 nM CNT) in 4-(2-hydroxyethyl)-1-piperazineethanesulfonic acid buffer (HEPES, 17 mM, pH 7.5) were prepared for imaging by heating (65 °C, 10 min), cooling to RT, combining with a similarly heated $MgCl_2$ solution (6 mM), and depositing (10 $\mu$L) onto freshly cleaved ruby mica (Spruce Pine Mica Company, Spruce Pine, NC). After ∼30 s of incubation, the mica was rinsed three times by adding several drops of water, blotted, and evaporated under a nitrogen stream. All concentrations above are reported for the final deposition solution.

Samples of CNTs suspended by the adsorption of SDS in the absence of DNA (CNT−SDS) were prepared by drying (opening to air for 24 h) the CNT gel before bath sonication (30 min) in a 1% SDS aqueous solution. CNT−SDS samples were deposited onto mica as described above (giving final concentrations of 0.1% SDS, 17 mM HEPES, and 6 mM $MgCl_2$).

Image analysis of CNT−DNA and CNT−SDS was performed using Nanoscope III v5.12 software (Veeco Instruments) and Image SXM (S. D. Barrett, http://www.ImageSXM.org.uk). Measurements were made for CNTs longer than 50 nm (except for length measurements), excluding CNTs that were not visible (i.e., covered by carbonaceous impurities or large masses of surfactant), and are reported as the Gaussian center ± 1 standard deviation (calculated using Origin, OriginLab Corp., Northampton, MA).

Quantum dot (QD) labeling studies were performed with core/shell CdSe/ZnS ($\lambda_{em}$ = 540 nm) EviDots from Evident Technologies (Troy, NY). A literature procedure was followed to substitute the trioctylphosphine oxide ligands with mercaptoacetic acid to yield water-soluble QDs,[34] and the QD concentration was determined spectrophotometrically from an extinction coefficient provided by Evident Technologies. To form CNT−DNA conjugates with QDs, CNT−DNA made with a thiolated oligonucleotide (3.0 mg/L or ∼18 nM CNT) was incubated with 2.2 $\mu$M QDs at RT for 24 h. This solution was deposited onto mica for imaging without heating, but otherwise as described above (with final concentrations of 2.7 mg/L or ∼16 nM CNT, 17 mM HEPES, 6 mM $MgCl_2$, and 2.0 $\mu$M QD, which was chosen to optimize the QD surface coverage on the mica). The CNTs used in QD labeling experiments were wrapped with 5′-biotin-$(GT)_{30}$ (CNT−biotin), 5′-thiol-$(GT)_{30}$ (CNT−thiol), and 5′,3′-dithiol-$(GT)_{30}$ (CNT−dithiol) 60-mers or with the 5′-thiol-$(GT)_{60}$ 120-mer.

In image analysis, "QD-sized objects" refer to all round objects of heights > 1 nm in contact with the CNT. Measurements of the distance between QD-sized objects on CNTs wrapped with thiolated oligonucleotide (reported as the Gaussian center ± 1 standard deviation) were made from the center of each object and excluded objects in contact with each other. The number of QD-sized objects per CNT (reported as the average ± 1 standard deviation for three

(20) Chou, S. G.; DeCamp, M. F.; Jiang, J.; Samsonidze, G. G.; Barros, E. B.; Plentz, F.; Jorio, A.; Zheng, M.; Onoa, G. B.; Semke, E. D.; Tokmakoff, A.; Saito, R.; Dresselhaus, G.; Dresselhaus, M. S. *Phys. Rev. B* **2005**, *72*, 195415/1−8.
(21) Lu, Y.; Bangsaruntip, S.; Wang, X.; Zhang, L.; Nishi, Y.; Dai, H. *J. Am. Chem. Soc.* **2006**, *128*, 3518–3519.
(22) Staii, C.; Chen, M.; Gelperin, A.; Johnson, A. T. *Nano Lett.* **2005**, *5*, 1774–1778.
(23) Zheng, M.; Jagota, A.; Strano, M. S.; Santos, A. P.; Barone, P.; Chou, S. G.; Diner, B. A.; Dresselhaus, M. S.; McLean, R. S.; Onoa, G. B.; Samsonidze, G. G.; Semke, E. D.; Usrey, M.; Walls, D. J. *Science* **2003**, *302*, 1545–1548.
(24) Zheng, M.; Semke, E. D. *J. Am. Chem. Soc.* **2007**, *129*, 6084–6085.
(25) Huang, X.; McLean, R. S.; Zheng, M. *Anal. Chem.* **2005**, *77*, 6225–6228.
(26) Arnold, M. S.; Stupp, S. I.; Hersam, M. C. *Nano Lett.* **2005**, *5*, 713–718.
(27) Chen, Y.; Liu, H.; Ye, T.; Kim, J.; Mao, C. *J. Am. Chem. Soc.* **2007**, *129*, 8696–8697.
(28) Zuccheri, G.; Brucale, M.; Samori, B. *Small* **2005**, *1*, 590–592.
(29) Manohar, S.; Tang, T.; Jagota, A. *J. Phys. Chem. C* **2007**, *111*, 17835–17845.
(30) Johnson, R. R.; Johnson, A. T. C.; Klein, M. L. *Nano Lett.* **2008**, *8*, 69–75.
(31) Enyashin, A. N.; Gemming, S.; Seifert, G. *Nanotechnology* **2007**, *18*, 245702–245712.
(32) Lustig, S. R.; Jagota, A.; Khripin, C.; Zheng, M. *J. Phys. Chem. B* **2005**, *109*, 2559–2566.
(33) Bachilo, S. M.; Balzano, L.; Herrera, J. E.; Pompeo, F.; Resasco, D. E.; Weisman, R. B. *J. Am. Chem. Soc.* **2003**, *125*, 11186–11187.
(34) Patolsky, F.; Gill, R.; Weizmann, Y.; Mokari, T.; Banin, U.; Willner, I. *J. Am. Chem. Soc.* **2003**, *125*, 13918–13919.

experiments) was determined for CNTs longer than 100 nm, and a two-tailed one-way ANOVA with Bonferroni's posthoc test ($p < 0.05$) was performed to compare the data for each experimental group using Kaleidagraph (Synergy Software, Reading, PA).

**Calculations and Modeling.** CNTs built in the Microscope Simulator program[35] (http://www.cs.unc.edu/research/nano/cismm/) and used for calculations were 0.8 nm in diameter, which is consistent with both the height of unwrapped nanotubes observed in AFM images and the reported diameter of CoMoCAT CNTs.[33] In CNT−DNA, the ssDNA backbone is ~0.5 nm above and below the nanotube due to $\pi$-stacking of bases on the CNT surface;[29,31] ssDNA was therefore modeled as a helical pipe of 0.5-nm diameter tangent to the CNT. An AFM tip radius of 8 nm and a cone angle of 20° were used in all simulations.[35]

To determine the number of turns made by one oligonucleotide wrapped helically around a nanotube, the ssDNA was treated as a wire positioned at the DNA backbone. This wire is helically wrapped around a cylinder of 1.8-nm diameter (because the ssDNA backbone is ~0.5 nm above and below the 0.8-nm diameter CNT[29,31]). The ssDNA length ($L$), its wrapping pitch ($h$), or the number of turns it makes around the cylinder ($n$) can be easily calculated when given the other two parameters. A cylinder (of diameter $d$) wrapped with one turn of ssDNA can be formed by rolling a rectangle so that its diagonal makes exactly one helical turn around the cylinder; the length ($l$) of that diagonal (i.e., one turn of the ssDNA) is then given by the Pythagorean Theorem. The total length of the ssDNA is $l$ times the number of turns around the cylinder: $L = nl = n\sqrt{[h^2 + (\pi d)^2]}$. The length of an oligonucleotide was calculated by assuming a distance of 0.7 nm between phosphorus atoms on the ssDNA backbone ($L = 42$ nm for one 60-mer). This distance is found in ssDNA adopting a C2′ *endo* conformation[36] (and can be calculated by treating one strand of a double helix with a 3.4-nm pitch as a wire on a cylinder of 2-nm diameter).

## Results

**Measurements of the CNT−DNA Surface Pattern.** CNTs produced by the CoMoCAT process[33] were wrapped with a single-stranded guanine-thymine deoxyribooligonucleotide, $(GT)_{30}$. The CNT−$(GT)_{30}$ length distribution measured by AFM shows a trend to three different lengths (47 ± 45 nm, 172 ± 56 nm, and 311 ± 105 nm) with an average length of 144 ± 112 nm ($n > 800$), which is comparable to that reported for CNT−DNA made with HiPco-process CNTs via a similar protocol.[23]

AFM imaging reveals a regular pattern on the CNT−DNA surface[23] consisting of peaks and valleys in height along the length of each tube, as well as corresponding shifts in the phase of the cantilever oscillation. This uniform pattern was observed along the entire length of all DNA-wrapped CNTs (Figure 1). The nanotube height above the mica substrate was 1.2 ± 0.2 nm at the peaks and 0.8 ± 0.2 nm at the valleys comprising the surface pattern. The width of the peaks along the CNT surface was 12 ± 5 nm, and the pitch (i.e., peak-to-peak distance) was 14 ± 5 nm. For comparison, CNT−$(GT)_{30}$ made from HiPco CNTs (which have a larger diameter than CNTs produced via CoMoCAT[7,33]) have an average height of ~2 nm and a pitch of ~18 nm.[23] Along with CNT−DNA, images show globular objects attributed to carbonaceous impurities from the CNT source material[25] (Figure 1A).

**Effect of the DNA Sequence.** The $(GT)_{30}$ sequence was studied because of a previous report modeling CNT−$(GT)_{30}$ as a special case, giving rise to a much more uniform AFM surface pattern than CNTs wrapped with other sequences.[23] For comparison to $(GT)_{30}$-wrapped CNTs, we imaged CNTs wrapped with an entirely thymine sequence of the same length, $T_{60}$. Under our AFM conditions, we observed a regular surface pattern for CNT−$T_{60}$. This pattern was indistinguishable from that of CNT−$(GT)_{30}$ and similarly prevalent along the lengths of the CNTs (Figure 2). The CNT−$T_{60}$ pitch (14 ± 5 nm) and peak width (12 ± 5 nm) along the nanotube were identical to that of CNT−$(GT)_{30}$.

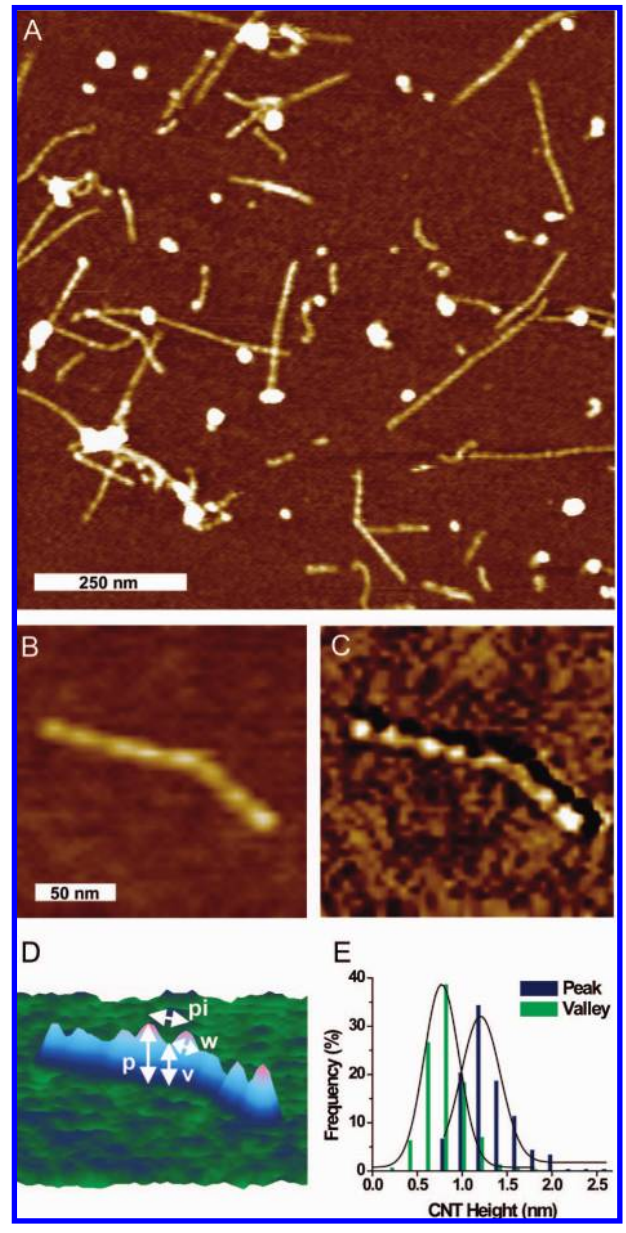


***Figure 1.*** (A) AFM height image of CNTs wrapped with $(GT)_{30}$ oligonucleotide (5-nm scale). (B) Height image (5-nm scale) and (C) phase image (25° scale) of one representative CNT−DNA, along with (D) a 3D representation (1.7-nm scale) indicating the peak height (p), valley height (v), peak width (w), and pitch (pi) measurements. (E) Distributions of nanotube height measurements at peaks and valleys ($n = 300$ CNTs).

**Effect of the DNA Length.** CNTs wrapped with 30-, 60-, and 120-mer oligonucleotides of entirely thymine bases were compared to examine the effect of oligonucleotide length on CNT−DNA structure. Images of CNT−$T_{30}$ and CNT−$T_{120}$ revealed a surface pattern similar to that observed for the two

(35) Varadhan, G.; Robinett, W.; Erie, D.; Taylor II, R. M. *SPIE* **2002**, *4665*, 116–124.
(36) Sarma, R. H., Ed. *Nucleic Acid Geometry and Dynamics*; Pergamon Press: Elmsford, NY, 1980.

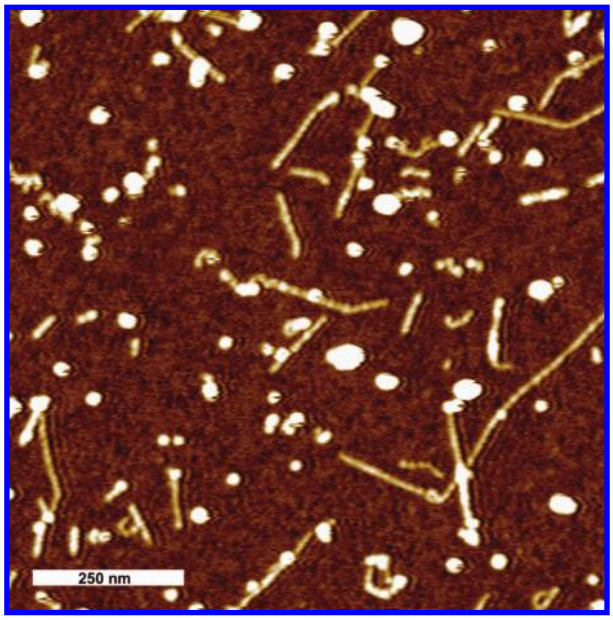


***Figure 2.*** AFM height image of CNTs wrapped with $T_{60}$ oligonucleotide, showing the surface pattern along the length of the CNTs and its prevalence (5-nm scale).

60-mers, $(GT)_{30}$ and $T_{60}$ (Figure 3). The peak width and pitch measurements of CNTs wrapped with $T_{30}$, $T_{60}$, $T_{120}$, and $(GT)_{30}$ were all within one standard deviation (Figure 3G, H). The pitch ($13 \pm 5$ nm) and peak width ($13 \pm 4$ nm) of CNT−$T_{120}$ were similar to that of the 60-mer-wrapped CNTs, while the pitch ($10 \pm 4$ nm) and peak width ($11 \pm 4$ nm) of CNT−$T_{30}$ were slightly shorter.

**Quantum Dot Labeling of the Wrapping DNA.** To identify the location of oligonucleotides on CNT−DNA, we sought to label the wrapping DNA in a manner recognizable by AFM. We attached mercaptoacetic acid stabilized QDs (of CdSe core and ZnS shell) having an ~2.4-nm diameter to CNTs wrapped with thiolated oligonucleotide. The resulting CNT−DNA−QD conjugates were stable in aqueous solution, and the QDs provided a convenient size marker in AFM images to identify the location of DNA on CNTs (Figure 4A). The DNA-bound QDs were observed to be positioned along the regular surface pattern of CNT−DNA, localized on the peaks in height. For CNTs wrapped with 5′-modified 60-mers, QDs bound near each other on the same nanotube showed a regular spacing of ~40 nm ($43 \pm 20$ nm for the shortest Gaussian population of QD-to-QD distances), suggesting a 40-nm interval along the nanotube between the thiol groups of different oligonucleotides. The QD-to-QD distance on CNTs wrapped with 5′-thiolated 120-mers was ~60 nm ($63 \pm 26$ nm for the shortest Gaussian population of QD-to-QD distances), suggesting a larger spacing between thiol groups of the modified 120-mers.

To ensure that QD binding was selective for the thiol groups on the wrapping DNA, CNTs were wrapped with $(GT)_{30}$ modified to contain zero (CNT−biotin), one (CNT−thiol), or two (CNT−dithiol) thiols per strand and then incubated in solution with (or without) QDs (24 h, RT). AFM images were collected, and the number of QD-sized objects (round objects of height > 1 nm) observed per nanotube was counted; this count included both QDs and the carbonaceous impurities that were observed in all CNT−DNA images. The average number of QD-sized objects observed per CNT for each experimental group is shown in Figure 4B.

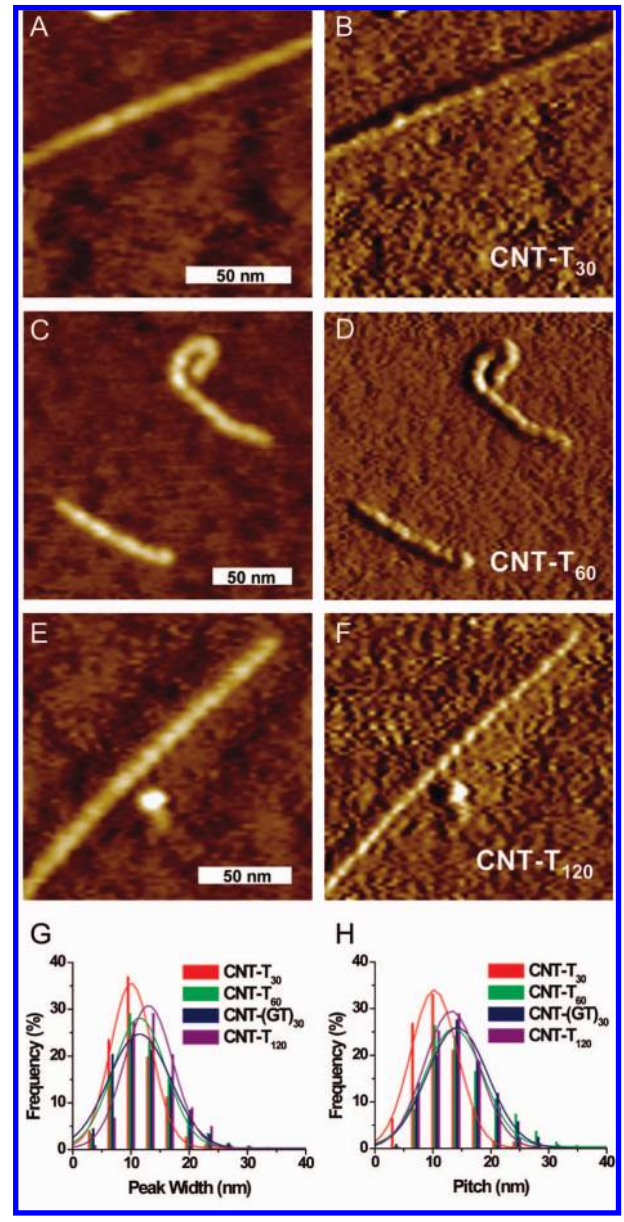


***Figure 3.*** (A−F) AFM height (left) and phase (right) images of representative CNTs wrapped with thymine oligonucleotide sequences of 30-, 60-, and 120-base length (shown with 5-nm height scales and phase scales of 8°, 25°, and 10°, respectively). (G) Peak width along the CNT surface and (H) pitch (peak-to-peak distance) distributions for CNTs wrapped with $T_{30}$, $T_{60}$, $(GT)_{30}$, and $T_{120}$ oligonucleotides ($n > 500$).

The number of objects/CNT for the nonthiolated control (CNT−biotin) in the presence of QDs ($0.4 \pm 0.1$) was *not* significantly different from that found in the absence of QDs ($0.4 \pm 0.05$). However, when one thiol was present per strand of the wrapping DNA (CNT−thiol), the number of objects/CNT in the presence of QDs ($0.9 \pm 0.3$) was significantly increased compared to that in their absence ($0.4 \pm 0.1$). A significant increase was likewise observed for CNTs wrapped with oligonucleotides containing two thiols per strand (CNT−dithiol, which had $0.4 \pm 0.1$ objects/CNT in the absence of QDs, but $1.2 \pm 0.2$ objects/CNT in their presence). Furthermore, significantly more objects were observed per CNT for CNT−dithiol than for CNT−thiol. The data were also analyzed in this manner with respect to the location of objects on the CNT; the significant differences reported above were also true when considering only

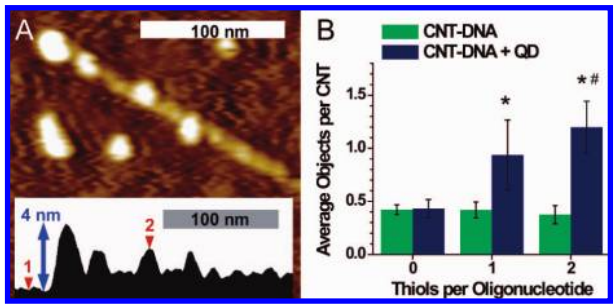


***Figure 4.*** (A) AFM image of a CNT wrapped with a thiolated oligonucleotide then incubated with QDs in solution for 24 h at RT (5-nm height scale). Inset: cross section of this CNT, where position 1 indicates the mica substrate and position 2 indicates a QD bound to CNT−DNA. (B) Average number of QD-sized objects observed per nanotube for CNTs wrapped with DNA containing 0, 1, or 2 thiols per strand (with and without QD incubation). Data are the average of three experiments ($n = 500$ CNTs per group, per experiment); error bars show the standard deviations of the three experiments. Significant increases compared to 0 thiols (*) and to 1 thiol (#) are indicated for data in the presence of QDs.

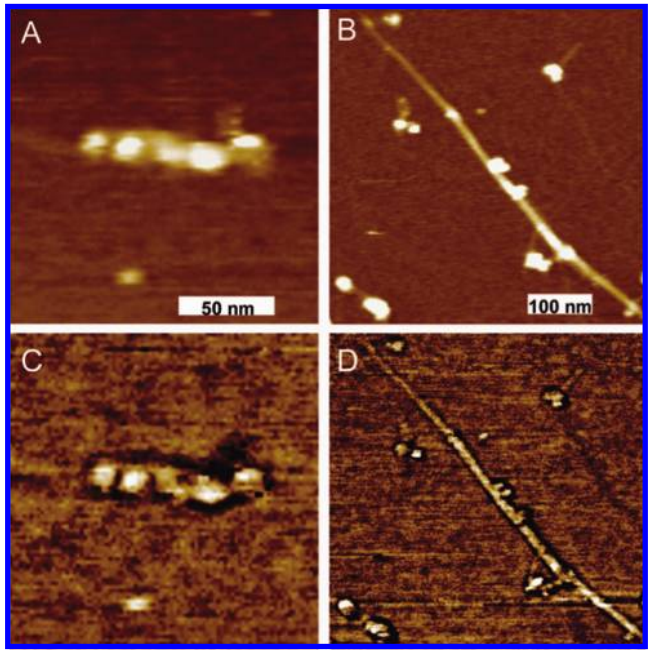


***Figure 5.*** Nanotubes representative of the different structures observed for SDS-suspended CNTs (in the absence of DNA). AFM height (top, 5-nm scale) and phase (bottom, 10° scale) images of CNTs exhibiting (A, C) patterned and (B, D) irregular SDS coverage. These two nanotubes were observed in the same 1-$\mu$m AFM image.

those objects observed at the nanotube ends or only objects along the CNT sidewalls.

**Comparison to CNT−SDS.** To study CNT structure without the presence of DNA, we suspended CNTs in water containing 1% SDS (which was necessitated by the aggregated state of as-produced CNTs) and imaged the resulting CNT−SDS material via AFM. Like ssDNA, SDS is an amphiphilic molecule capable of dispersing CNTs in water;[6] however, the structure of SDS surfactant on CNTs differed from that of DNA on CNTs. While SDS was sometimes ordered into a pattern along the CNT, irregular surface coverage was also observed (Figure 5).

Patterned organization of SDS was only observed on short (~100 nm or less) CNTs or segments of CNTs (Figure 5A,C) and was less common than irregular organization; the patterned structure accounted for only ~25% of surfactant coverage on CNTs. The pitch (18 ± 6 nm) and peak width (19 ± 5 nm) of this surfactant pattern were larger than that of CNT−DNA ($n > 600$). The prominent CNT−SDS peaks were taller (3.8 ± 1.0 nm) and more varied in height compared to CNT−DNA, and valley measurements were taller (1.4 ± 0.7 nm) than those for the bare CNT, indicating the presence of SDS even at the valleys of the pattern ($n = 300$).

While no regions of uncovered CNT were observed for CNT−DNA, areas of bare CNT were present on CNT−SDS tubes exhibiting irregular structures (Figure 5B,D). The CNT height at these uncovered regions was 0.8 ± 0.3 nm ($n = 300$), which agrees with both the valley heights observed for CNT−DNA and the reported diameter of CoMoCAT CNTs.[33] To investigate whether surfactant was removed from the nanotubes during AFM sample preparation, we compared our method employing brief rinsing of the deposited CNT−SDS to a preparation with extensive (10-fold increased) rinsing. The percentage of uncovered nanotube surface ranged from 5 to 39% in both procedures, and the extent of rinsing did not cause a statistical difference in the mean percentage of uncovered CNT.

## Discussion

**QDs reveal DNA location along the entire CNT.** Variation in AFM phase images is caused by differing interactions between the sample and the AFM tip. Therefore, the observation of a regular surface pattern along CNT−DNA in phase as well as height images suggests that the pattern is formed by different materials, CNT and DNA. The height at the valleys of the pattern is consistent with unwrapped CoMoCAT CNTs, which are on average 0.81 nm in diameter.[33] The difference between the peak and valley heights of the pattern (~0.4 nm) is attributed to a single layer of ssDNA, in agreement with the predicted height of ~0.5 nm for $\pi$-stacked ssDNA on a CNT.[29,31] These height data suggest that oligonucleotides interact with the CNT sidewalls, forming peaks where they are bound and leaving valleys whose heights reflect the bare nanotube. A single population was observed in the distribution of CNT−DNA peak heights (Figure 1E), suggesting that DNA is only present in this single-layer coverage on the CNT surface. Assignment of the regular CNT−DNA surface pattern to the presence of DNA is supported by the absence of the pattern in images of surfactant-suspended CNTs.

This analysis of the origin of the CNT−DNA AFM pattern is corroborated by QD labeling of the DNA. DNA-bound QDs were positioned along the regular surface pattern of the nanotube, localized on the peaks in height. Nonspecific binding of QDs to CNT−DNA was not appreciable, and QDs were observed to bind selectively to thiolated DNA both at the nanotube ends and along the sidewalls, identifying the location of oligonucleotide along the entire CNT. *This observation is the first direct evidence of the oligonucleotide location on DNA-wrapped CNTs and suggests that the AFM surface peaks result from the DNA.* The persistence of the surface pattern along the entire CNT (regardless of the length of the wrapping DNA) without regions of unwrapped nanotube suggests that the CNT−DNA has nearly complete DNA coverage. The oligonucleotides must be closely arranged along the CNT, with more oligonucleotides needed per CNT for shorter DNA (or for longer CNTs). This close arrangement of DNA strands likely serves to minimize the unfavorable interaction of the hydrophobic CNT surface with the aqueous solution.

These findings have important implications for future applications of the CNT−DNA nanomaterial. For instance, the

lack of unwrapped CNT regions may serve to limit nonspecific binding when CNT−DNA is employed in biosensing. In schemes seeking to derivatize the DNA, the high coverage of oligonucleotides would allow for a high density of functional moieties per CNT.

**Turns of helically wrapped DNA produce the CNT−DNA surface pattern.** The Microscope Simulator program[35] was employed to build models of the DNA structure on a CNT and to simulate the height image that would be produced for each model by an AFM tip. CNTs and ssDNA can interact in a stable, organized manner by helical wrapping of ssDNA around CNTs.[17,29–32,37] To model this interaction, a CNT (of 0.8-nm diameter) was wrapped with a helical pipe (of 0.5-nm diameter, tangent to the CNT) representing the ssDNA. We considered situations in which each peak in CNT−DNA height comprising the regular AFM pattern could arise from (1) each turn of helically wrapped DNA around the CNT or (2) each oligonucleotide on the CNT. The evidence needed to evaluate the appropriateness of these models was provided by images of CNTs wrapped with different lengths of DNA.

In the case of each turn of helically wrapped DNA around the CNT generating one peak in the AFM height image, the pitch of the AFM surface pattern is equal to the wrapping pitch of the DNA (and the peak width is the width of each DNA turn on the top of the CNT). To model this structure, a CNT was helically wrapped by 60-mer oligonucleotides with a 14-nm pitch (equivalent to the pitch observed by AFM). A 60-mer at this pitch was calculated to turn ∼2.8 times around the CNT, covering a nanotube length of ∼40 nm (see Experimental Section). This CNT length is considerably less than the average observed for our sample, implying that several oligonucleotides (3−4 oligonucleotides for a CNT of average length) are bound per CNT in an end-to-end manner. These oligonucleotides must be closely arranged along the CNT to produce the observed AFM pattern, which covers the entire CNT without any unwrapped areas.

Simulation of a CNT covered by two 60-mers positioned end-to-end with a 14-nm wrapping pitch generated an AFM image consistent with the regular surface pattern observed experimentally (Figure 6A). In this model, wrapping with longer oligonucleotides means more of the CNT is covered per strand, but the same total length of CNT can be covered by wrapping with multiple short oligonucleotides closely arranged along the CNT. This effect can be seen in Figure 6A by viewing the two 60-mers composing the DNA wrap as a single 120-mer or as four adjacent 30-mers; each instance produces the same AFM surface pattern. Therefore, the lack of a dramatic effect of oligonucleotide length on the AFM surface pattern (of CNT−$T_{30}$, −$T_{60}$, and −$T_{120}$) supports the assignment of one AFM surface peak to each turn of the wrapped DNA.

This assignment is corroborated by the regular spacing of ∼40 nm observed between the centers of QDs bound near one another on CNTs wrapped by monothiolated 60-mers because each 60-mer at a 14-nm wrapping pitch was calculated to cover a CNT length of ∼40 nm. Our observation of an ∼60-nm spacing between QDs on CNTs wrapped by thiolated 120-mers is consistent with the expected ∼80-nm spacing due to the large variation (±26 nm) introduced by wrapping pitch variation and the size of the QDs. Comparison of the QD spacing measurement to the length of a wrapped oligonucleotide assumes

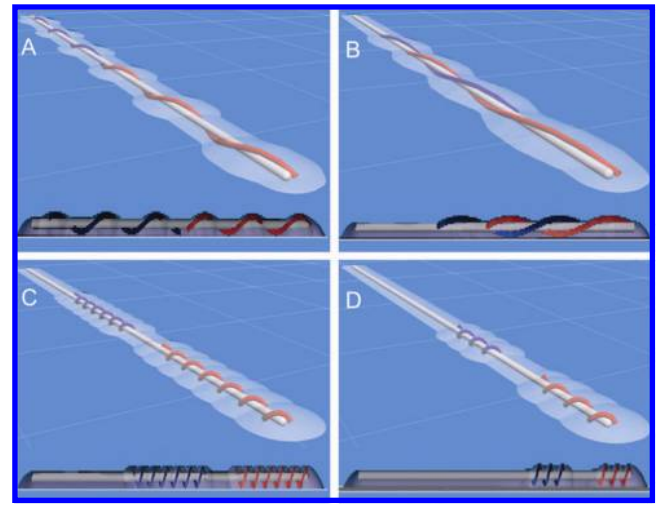


***Figure 6.*** Simulated AFM images of CNT−DNA models (for a CNT of 0.8-nm diameter and 80-nm length). (A) Each turn of the DNA around the CNT (14-nm pitch) generates one surface peak in the AFM image; the DNA is colored to show two 60-mers, but the same image results from wrapping with one 120-mer or four adjacent 30-mers. (B) Each turn of the DNA around the CNT (28-nm pitch) generates one surface peak in the AFM image; the colors indicate two interlaced 60-mers offset from each other by 14 nm. (C) Each oligonucleotide generates one surface peak in the AFM image; the colors indicate two 60-mers at a 3.4-nm wrapping pitch. (D) Case shown in (C) for two 30-mers.

oligonucleotide attachment to the center of each QD; variation in the actual position of attachment limits the usefulness of the QD as an exact marker for the end of the oligonucleotide. The larger spacing observed between QDs on CNTs wrapped with 120-mers compared to 60-mers supports the model proposed in Figure 6A.

Two interlaced DNA helices with a 28-nm wrapping pitch that are offset from each other by 14 nm would result in an AFM surface pattern with a 14-nm pitch (Figure 6B). However, our data and recent molecular dynamics simulations revealing the decreased stability of larger DNA wrapping pitches[30] suggest that adjacent oligonucleotides on a CNT do not helically intertwine. The larger wrapping pitch of the DNA in Figure 6B results in a less distinct AFM surface pattern than that produced by the noninterlaced model in Figure 6A, and instances where the helices are not offset by exactly 14 nm would introduce greater variability in the AFM pitch than we observed experimentally.

An alternate explanation for the CNT−DNA surface pattern observed via AFM is that each height peak results from one bound oligonucleotide, making the pitch equal to the distance between the centers of adjacent oligonucleotides and the peak width equal to the length of one oligonucleotide. This case requires DNA wrapping with too small a pitch for the individual turns to be distinguished by the AFM tip and gaps between oligonucleotides to produce a regular pattern in CNT−DNA height. The model in Figure 6C meets these requirements and was constructed with the same wrapping pitch as that in a DNA double helix (3.4 nm, allowing a 60-mer to make 6.4 turns around the CNT and cover a CNT length of ∼20 nm). This model produces an AFM image with a periodic variation in height. However, the model predicts a dramatic effect of the oligonucleotide length, where the peak width of CNT−$T_{120}$ would be double that of CNT−$T_{60}$ and quadruple that of CNT−$T_{30}$ (and the pitch would also vary); these effects are shown in Figure 6C,D. No such length effects were observed

(37) Gigliotti, B.; Sakizzie, B.; Bethune, D. S.; Shelby, R. M.; Cha, J. N. *Nano Lett.* **2006**, *6*, 159–164.

experimentally, supporting the wrapping model in Figure 6A over that in 6C,D.

Overall, our AFM measurements and modeling suggest that the observed pitch of the CNT−DNA surface pattern in AFM images corresponds to the pitch of the wrapping DNA for oligonucleotides closely arranged, but not intertwined, on the CNT surface. Since multiple oligonucleotides are present per CNT, the pitch distribution may include not only turn-to-turn measurements of wrapped oligonucleotides but also any distances between two adjacent oligonucleotides. This occurrence may be responsible for the slightly shorter pitch measurement of CNTs wrapped with the shortest oligonucleotide (CNT−$T_{30}$). As the 30-mer can only execute one complete turn around the CNT (1.8 turns versus 2.8 turns for $T_{60}$ and 5.9 turns for $T_{120}$), its pitch measurement would be the most influenced by measurements of the spacing between oligonucleotides. Alternatively, the inability of the 30-mer to make more than one complete turn around the CNT might favor a shorter wrapping pitch to increase the energetic stability of the hybrid (as suggested by molecular dynamics work[30]). It is likely that spacing measurements do not have a substantial impact on AFM pitch measurements due to the narrow pitch distribution (±4 or 5 nm) observed, which indicates the regularity of the DNA organization along the CNT.

Modeling predicts an optimum DNA wrapping pitch for any given CNT−DNA hybrid, dependent on the physical and electronic characteristics of the CNT.[29] The CoMoCAT CNTs used to prepare our CNT−DNA samples have a narrow distribution of diameters and (*n*,*m*) types,[33] which is reflected in the narrow distribution we observed for AFM pitch measurements. The DNA wrapping pitch of individual CNT−DNA hybrids can be determined through measurement of the surface pattern pitch in AFM images. This connection is of practical importance in the development of ion exchange chromatography as a means to separate CNT−DNA according to CNT type,[23,24] since the DNA wrapping pitch is the primary factor in controlling the separation.[32]

**CNT−DNA surface pattern is independent of the DNA sequence.** No significant impact of the oligonucleotide sequence on the structure of CNT−DNA was observed for the 60-mers studied, $(GT)_{30}$ and $T_{60}$. This finding is consistent with a report that CNTs suspended by a random, long ssDNA sequence exhibited a periodic wrapping structure[37] and with molecular dynamics results indicating that the forces driving both the DNA-to-CNT adhesion and the helical wrapping are sequence-independent.[30] However, although the wrapping oligonucleotide sequence does not affect the CNT−DNA hybrid structure observed via AFM, it does play a role in determining CNT−DNA properties. Notably, CNTs wrapped with different DNA sequences vary in their ability to be sorted (according to electronic character and diameter) by ion exchange chromatography.[23] Sorting via this technique is attributed to differences in the effective linear charge density (which is sensitive to CNT electronic character and diameter) of CNT−DNA hybrids formed from different (*n*,*m*) types of CNTs.[23,32] CNTs wrapped with oligonucleotides of alternating GT sequence produce the best separation (including better separation compared to T sequences),[23] but our AFM observations suggest that this difference in properties is not the result of a difference in DNA wrapping structure. Others have suggested that the varying success of different wrapping sequences in sorting CNT−DNA may result from sequence-dependent effects that do not impact the CNT−DNA structure (such as solvation or interactions between nucleotides).[30]

**SDS structure on CNTs differs from that of DNA.** The uniformity of the CNT−DNA pattern contrasts with the variety of the structures observed for CNT−SDS. While conditions such as the solution surfactant concentration and temperature are expected to affect CNT−SDS organization, nanotubes from the same solutions displayed different surfactant structures (Figure 5). The representative CNT in Figure 5B, D bears irregularly adsorbed masses of surfactant, along with smooth surfactant layers of varying height. These smooth layers suggest an organization based upon either cylindrical micelle encapsulation of the CNT[6,38] or wrapping by a hemicylindrical micelle.[39] In contrast, the pattern observed for nanotubes such as that in Figure 5A, C suggests a single-file adsorption of surfactant aggregates. While these types of CNT−SDS displayed more consistent organization, the irregular structures predominated.

Surfactants offer advantages in CNT separation procedures due to their low cost, diverse properties, and reversible adsorption to CNTs. An effective technique for sorting surfactant-dispersed CNTs according to CNT electronic type and diameter is density-gradient ultracentrifugation.[40] However, effective separation is dependent upon the formation of consistent surfactant structures that only vary (in orientation, packing density, hydration, etc.) according to the properties of each individual CNT. Therefore, careful choice of surfactant and preparation of suspensions to give individually dispersed CNTs with consistent surfactant organization are essential to successful CNT sorting. The inconsistent structures we observed for CNT−SDS may explain their poor separation performance[40] in density differentiation experiments compared to CNTs dispersed with bile salts. In contrast to the CNT−SDS structure, the uniform organization of CNT−DNA suggests an advantage of DNA wrapping in CNT sorting strategies.

**CNT−DNA−QD conjugates demonstrate noncovalent QD attachment to CNTs.** The significant increase observed in the number of objects/CNT upon QD incubation only when thiols were present on the wrapping DNA suggests that QD binding to CNT−DNA occurs selectively at the thiol groups. The coincubation of QDs and CNTs wrapped by thiolated DNA did not noticeably affect nanotube solubility; no CNT precipitation was observed over a period of several weeks. In contrast, attempts to label CNTs wrapped by biotinylated DNA with streptavidin (by adding a protein solution to CNT−biotin) resulted in immediate nanotube aggregation, with the degree of aggregation dependent upon the concentration of streptavidin added. In QD labeling experiments, on the other hand, we found oligonucleotides capable of interacting with both a QD and a CNT simultaneously. QD binding is assumed to occur when the thiolated terminus of the CNT-bound oligonucleotide binds to the QD ZnS shell and acts as a functionalized capping ligand, linking the QD to the CNT.

To compare the number of available thiol groups to the number of bound QDs, we calculated the approximate number of QDs bound per CNT (by subtracting the average number of QD-sized objects per CNT without QD incubation from that with QD incubation). This calculation gives a reasonable

(38) Matarredona, O.; Rhoads, H.; Li, Z.; Harwell, J. H.; Balzano, L.; Resasco, D. E. *J. Phys. Chem. B* **2003**, *107*, 13357–13367.
(39) Richard, C.; Balavoine, F.; Schultz, P.; Ebbesen, T. W.; Mioskowski, C. *Science* **2003**, *300*, 775–778.
(40) Arnold, M. S.; Green, A. A.; Hulvat, J. F.; Stupp, S. I.; Hersam, M. C. *Nat. Nanotechnol.* **2006**, *1*, 60–65.

representation of the actual number of QDs/CNT due to the constant background of ~0.4 objects/CNT observed for all of the control groups (Figure 4B). After incubation with QDs, the nonthiolated (CNT−biotin) control had approximately zero (0.01) QDs/CNT, while CNT−thiol had 0.5 QDs/CNT, and CNT−dithiol had 0.8 QDs/CNT. Although 3−4 oligonucleotides were calculated to cover a CNT of average length, CNTs wrapped with monothiolated oligonucleotides had an average of only 0.5 QDs/CNT; therefore, at the concentrations of CNT−DNA and QDs used for AFM imaging (an excess of QDs), we did not observe QDs bound to every thiolated oligonucleotide strand. This may result from the thiol groups of some wrapped oligonucleotides not being fully accessible to QDs in solution.

Both QDs and CNTs are envisioned for future applications such as biological imaging and sensing.[2–4,41] QDs and single-walled CNTs have been combined through covalent methods[42] and noncovalent strategies such as electrostatic interactions[43] and $\pi$-stacking.[44] Our QD labeling experiments demonstrate a new method for binding QDs to CNTs and suggest the advantage of modifying the noncovalently wrapped ssDNA of CNT−DNA hybrids to selectively attach QDs in a manner that avoids covalent modification of the CNT surface.

## Conclusions

Measurements and modeling of the regular AFM pattern observed along CNT−DNA suggest that the hybrids are composed of oligonucleotides closely arranged end-to-end in a single layer along the entire nanotube surface, with each turn of the wrapped DNA generating one surface peak in the AFM images. Supporting this structural model, no significant impact of the oligonucleotide length was observed on the regular pitch of the surface pattern or on the width of the peaks along the CNT. QD labeling of CNTs wrapped with thiolated DNA identified the presence of DNA at the ends and along the entire sidewalls of the CNTs. This result and the prevalence of the CNT−DNA surface pattern imply nearly complete coverage of CNTs with DNA. The distance observed between QDs on a CNT was consistent with the CNT length calculated to be covered by one oligonucleotide wrapped at a 14-nm pitch, further supporting our model. The stable CNT−DNA−QD conjugates may prove to be a useful material due to the tunable fluorescence of QDs, and the use of QDs to label the DNA demonstrates the value of wrapping CNTs with modified oligonucleotides, which can confer desirable properties without covalently functionalizing (and thus altering the electronic properties of) the CNT. We observed no structural difference in the DNA wrapping pattern of CNTs solubilized with an alternating guanine-thymine DNA sequence versus an entirely thymine sequence, while the structure of CNT−DNA was found to be very different from that of CNTs suspended with SDS. Our findings of the DNA location and wrapping structure are expected to benefit the separation of CNT mixtures into homogeneous samples, which is a vital step in the majority of the envisioned applications for CNTs.

**Acknowledgment.** The authors acknowledge support from the U.S. Army (W911NF-05-0047, H.H.T.), National Institutes of Health (GM79480, D.A.E.), and American Cancer Society (RSG-05-047, D.A.E.). J.F.C. thanks the National Science Foundation for a graduate research fellowship and the U.S. Department of Education for a GAANN fellowship.

**Note Added after ASAP Publication.** Due to a production error, this paper was published ASAP July 16, 2008, before all corrections were incorporated. The final corrected version was published July 19, 2008.

**Supporting Information Available:** CNT−DNA preparation procedure, absorption spectrum, length distribution, and AFM phase images; CNT−SDS AFM height image and distributions of pitch, peak width, and height; CNT−DNA + QD AFM height image and distributions of the number of QD-sized objects per CNT and the distance between QD-sized objects on CNTs; complete author listing of ref 19. This material is available free of charge via the Internet at http://pubs.acs.org.

JA801720C

(41) Michalet, X.; Pinaud, F. F.; Bentolila, L. A.; Tsay, J. M.; Doose, S.; Li, J. J.; Sundaresan, G.; Wu, A. M.; Gambhir, S. S.; Weiss, S. *Science* **2005**, *307*, 538–544.
(42) Banerjee, S.; Wong, S. S. *Nano Lett.* **2002**, *2*, 195–200.
(43) Chaudhary, S.; Kim, J. H.; Singh, K. V.; Ozkan, M. *Nano Lett.* **2004**, *4*, 2415–2419.
(44) Li, Q.; Sun, B.; Kinloch, I. A.; Zhi, D.; Sirringhaus, H.; Windle, A. H. *Chem. Mater.* **2006**, *18*, 164–168.